# A Model for the Kinetics of Plasma Polymerization

**J. M. Tibbitt, R. Jensen, A. T. Bell,* and M. Shen**

*Department of Chemical Engineering, University of California, Berkeley, California 94720.* *Received August 16, 1976*

ABSTRACT: A general mechanism for the plasma polymerization of unsaturated hydrocarbon monomers in a flow reactor has been developed. Polymerization is postulated to occur via free-radical intermediates, formed as a result of electron–monomer collisions in the plasma. Material balances relating monomer and radical concentrations to reactor axial position were solved and used to predict the polymerization rate. By adjusting the magnitudes of the rate coefficients appearing in the model, good agreement was obtained between polymerization rates predicted by the model and those measured experimentally for a variety of unsaturated monomers. The magnitudes of the fitted rate coefficients describing the initiation of polymerization and gas phase oligomerization were found to be in good quantitative agreement with independently observed rated coefficients. Variations in the fitted rate coefficients with changes in polymerization conditions followed trends anticipated on the basis of elementary discharge physics.

Thin polymer films with unique physical and chemical characteristics can be produced by the passage of an organic monomer through the plasma produced in a low-pressure electric discharge. The process, referred to as plasma polymerization, is currently receiving attention as a means for preparing thin-film capacitors,[1] passivating coatings,[2] reverse osmosis membranes,[3,4] gas separation membranes,[5,6] optical wave guides,[7] and antireflecting coatings.[8] An added incentive for exploring plasma produced films is the recognition that such films are pinhole free, highly cross-linked, and insoluble in almost all organic solvents.

While there have been a number of studies devoted to the kinetics of plasma polymerization,[9–19] the mechanism by which polymerization occurs is still not well understood. There is general agreement among different authors that both homogeneous and heterogeneous reactions are involved and that collisions between plasma electrons and monomer molecules are required to initiate polymerization. However, the nature of the primary reaction intermediates remains a subject of discussion. An increasing body of evidence[13,16,17] suggests that free radicals play a dominant role but the possibility of polymerization by cationic species cannot be ruled out totally.[9,14,15,20]

Given the lack of a clear understanding of the polymerization mechanism it is not surprising that most authors have chosen to interpret the results of kinetic experiments only qualitatively. Notable exceptions of this are the studies of Denaro et al.,[11,12] Lam et al.,[18] and Poll[19] in which expressions are developed for describing the effects of the laboratory variables on the rate of polymer deposition.

In the present work a free-radical mechanism is proposed for the polymerization of unsaturated hydrocarbon monomers. After a simplification of the mechanism, conservation expressions are developed for the primary species participating in the reaction. The solutions to these equations are used in an expression for the polymer deposition rate. A comparison of experimental deposition rate data for a variety of monomers with predictions obtained from the model shows that the two are in reasonably good agreement for the conditions over which the model was tested. Furthermore, the rate coefficients obtained by fitting the model to the data are in reasonable quantitative agreement with independently observed rate coefficients.

## Theory

The geometry for which the model is to be developed is illustrated in Figure 1. Two parallel plate electrodes are used to sustain the discharge and to confine the gas flow. By imposing a sufficiently large electric field across the electrodes, the gas in the gap between them is broken down and made to conduct. The degree of ionization in the plasma produced this way is $10^{-5}$ to $10^{-6}$, and the number of free electrons and positive ions are nearly equal. For pressures below about 10 Torr the plasma will be in a nonequilibrium state[21] characterized by an electron temperature, $T_e$, which is 10 to 100 times greater than the ion temperature, $T_+$. Furthermore, the ion temperature will be nearly equal to the gas temperature $T_g$. Values of $T_e$ between $10^4$ and $10^5$ K and values of $T_g$ between 300 and 400 K are typical.

For the purposes of the model, the electron temperature and density will be assumed to be constant throughout the discharge. It will also be assumed that the gas flow is unidirectional and that the velocity profile is flat. Both the assumption of uniform plasma properties and plug flow have been used successfully in modeling other discharge systems.[21–23]

Polymerization will be assumed to proceed via a free-radical addition mechanism, based upon the following reasoning. First, it is recognized that at pressures of 1 Torr and above the free-radical concentrations in a nonequilibrium plasma are usually $10^3$ to $10^5$ higher than ion concentrations. As a consequence it can be shown[24] that free radical–molecule reactions occur at rates $10^1$ to $10^2$ faster than ion–molecule reactions. Second, it has been observed[25] that the addition of small amounts of haloforms to hydrocarbon monomers causes a significant acceleration of the monomer polymerization rate and a decrease in the H/C ratio of the polymer. These effects are most easily interpreted by assuming that free-halogen atoms released in the plasma enhance the free-radical population via hydrogen abstraction. A third reason for selecting a free-radical mechanism is the observation of high radical concentrations at the surfaces of polymers exposed to a plasma.[26,27] These surface free radicals are known to be able to react with unsaturated monomers.[28]

Table I illustrates the sequence of elementary reactions expected to occur when a hydrocarbon monomer enters the discharge. Polymerization is initiated through the collision of an electron with a monomer molecule. The products of these interactions, reactions 1–3, will include hydrogen atoms, hydrogen molecules, and free radicals. In addition, reactions 1 and 2 will yield a derivative monomer, which is more unsaturated than the original monomer. While it is possible that other types of initiation reactions can occur, reactions 1–3 are sufficient to describe the origins of the reactive intermediates, H· and $R\cdot_g$. Reaction 4 has been included as an initiation step to account for the fact that molecular hydrogen produced via reaction 1 can be dissociated to yield an additional source of atomic hydrogen.

The hydrogen atoms obtained from reactions 2 and 4 undergo a variety of reactions. Conversion to a free radical can occur by reaction 5 since $M_g$ and $M'_g$ are unsaturated. Gas-phase free radicals can also be formed by hydrogen abstraction processes such as reaction 19. Hydrogen atoms which diffuse

**Table I**
**Reaction Mechanism for Plasma Polymerization of Unsaturated Hydrocarbons[a]**

Initiation

1. $e + M_g \rightarrow M'_g + H_2 + e$
2. $e + M_g \rightarrow M'_g + 2H\cdot + e$
3. $e + M_g \rightarrow 2R\cdot_g + e$
4. $e + H_2 \rightarrow 2H\cdot + e$

Propagation (homogeneous)

5. $H\cdot + \begin{Bmatrix} M_g \\ M'_g \end{Bmatrix} \rightarrow R\cdot_{g_1}$
6. $R\cdot_{g_n} + \begin{Bmatrix} M_g \\ M'_g \end{Bmatrix} \rightarrow R\cdot_{g_{n+1}}$

Adsorption

7. $S + \begin{Bmatrix} M_g \\ M'_g \end{Bmatrix} \rightarrow \begin{Bmatrix} M_s \\ M'_s \end{Bmatrix}$
8. $S + H\cdot \rightarrow H\cdot_s$
9. $S + R\cdot_{g_n} \rightarrow R\cdot_{s_n}$

Propagation (heterogeneous)

10. $R\cdot_{s_n} + \begin{Bmatrix} M_g \\ M'_g \end{Bmatrix} \rightarrow R\cdot_{s_{n+1}}$
11. $R\cdot_{s_n} + \begin{Bmatrix} M_s \\ M'_s \end{Bmatrix} \rightarrow R\cdot_{s_{n+1}}$
12. $H\cdot_s + H\cdot \rightarrow H_2$

Termination

13. $R\cdot_{g_m} + H\cdot \rightarrow P_{g_m}$
14. $R\cdot_{g_m} + R\cdot_{g_n} \rightarrow P_{g_{m+n}}$
15. $R\cdot_{g_m} + R\cdot_{s_n} \rightarrow P_{s_{m+n}}$
16. $R\cdot_{s_m} + R\cdot_{s_n} \rightarrow P_{s_{m+n}}$

Reinitiation

17. $e + P_{g_{m+n}} \rightarrow R\cdot_{g_m} + R\cdot_{g_n}$
18. $P_s \xrightarrow{e, h\nu, I^+} R\cdot_{s_m} + R\cdot_{s_n}$
19. $H\cdot + P_{g_n} \rightarrow R\cdot_{g_n} + H_2$
20. $H\cdot + P_{s_n} \rightarrow R\cdot_{s_n} + H_2$

[a] $M_g$, primary monomer; $R\cdot_g$, gas phase free radical; $P_g$, gas phase oligomer; $M'_g$, derivative monomer; $R\cdot_s$, surface free radical; $P_s$, polymer fragment; $H\cdot$, hydrogen atom.

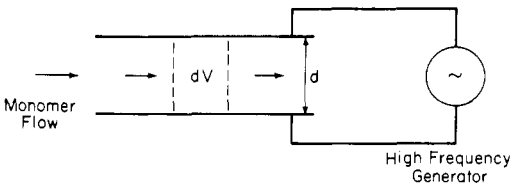


**Figure 1.** Postulated geometry for development of polymerization model.

to the surface of the electrodes can undergo heterogeneous reactions. Simple adsorption occurs by reaction 8. Reactions 12 and 13 are termination steps leading to the formation of molecular hydrogen in one case and a stable surface product in the second. Finally, reaction 20 illustrates the possibility that hydrogen atoms form surface free radicals by hydrogen abstraction.

Free radicals formed in the gas phase can undergo reactions which are quite similar to those for atomic hydrogen. Propagation to produce higher molecular weight radicals occurs via reaction 6. Radical–radical recombination is illustrated by reactions 13 and 14. The adsorption of a gas phase free radical can lead to the creation of a surface free radical via reaction 9, or to the termination of a surface free radical via reaction 15.

In addition to the processes just described for forming surface free radicals, additional surface radicals can be created by the interaction of energy fluxes from the plasma with the developing polymer surface (reaction 18). As sources of energy, one can consider photons, electrons, and ions. Once formed, surface free radicals can be lost by reaction with gas phase free radicals or by recombination between two surface free radicals.

To develop a model of the polymerization kinetics, it is necessary to simplify the reaction mechanism shown in Table I. We can begin by assuming that free-radical recombination in the gas phase, reactions 13 and 14, is not significant. For the pressures at which polymerization occurs (<10 Torr), loss of free radicals by diffusion and adsorption on solid surfaces is expected to predominate over gas-phase recombination. Further simplification of the mechanism is achieved by assuming that the generation of gas-phase free radicals by reactions 17 and 19 can be neglected by comparison with reactions 2–4. In support of both of these assumptions is the observation that oligomer concentrations in the gas phase are low compared to the monomer concentration.[29]

Next, we neglect the formation of surface free radicals by reaction 18, assuming that the origin of such radicals is the adsorption of gas-phase free radicals via reaction 9. The validity of this assumption will not be discussed here but will become apparent upon inspection of the results predicted by the model. Finally, reaction 20 will be neglected in recognition that reaction 12 already accounts for the formation of molecular hydrogen at the growing polymer surface.

Since the proposed mechanism involves a large variety of both gas and surface free radicals, to account in detail for each type of free radical would involve a complexity which is far beyond that necessary for the present. As a result we shall employ the usual assumption of polymerization kinetics that all radicals have equivalent reactivity.[30] Under this constraint reactions 5, 10, and 11 contribute to the consumption of monomer but do not alter the free-radical populations in the gas phase or on the growing polymer surface.

The rate of polymerization can now be expressed as

$$r_p = \frac{d}{2} k_6[M_g][R_g] + k_{10}[M_g][R_s] + k_{11}[M_s][R_s] \quad (1)$$

where $[X_g]$ and $[X_s]$ are the concentrations of species X in the gas phase and on the growing polymer surface, respectively, and $d$ is the spacing of the interelectrode gap (see Figure 1). The formulation of eq 1 assumes that monomer is consumed primarily in forming polymer and that the production of low molecular weight products is insignificant.[29]

The surface concentrations of monomer and free radicals appearing in eq 1 are assumed to be proportional to the gas-phase concentrations of these species. Thus,

$$[M_s] = K_M[M_g] \quad (2)$$

$$[R_s] = K_R[R_g] \quad (3)$$

Equations 2 and 3 are justified in the following way. The physical adsorption of monomer on nonradical surface sites is expected to be limited since all of the monomers used in this study have very high saturation vapor pressures. Under this condition the fractional surface coverage by adsorbed monomer is expected to be small and proportional to the monomer concentration in the gas phase. The surface free-radical concentration will be dictated by a balance between the rates of radical adsorption from the gas phase and radical recombination by processes such as reactions 15 and 16. By equating the rates of formation and loss of surface free radicals it is possible to obtain a relationship between the gas and surface free-radical concentrations. While the relation will not be linear in general, a linear expression, eq 3, has been assumed for the sake of convenience. Substitution of eq 2 and 3 into the expression for the rate of polymerization allows us to rewrite eq 1 as

$$r_p = \left(\frac{d}{2}k_6 + k_{10}K_R + k_{11}K_M K_R\right)[M_g][R_g] \quad (4)$$

The concentrations of monomer and free radicals appearing in eq 4 are determined by solving species conservation equations. These equations written for the differential volume $dV$ shown in Figure 1 are given below:

$$\frac{d(Q[R_g])}{dV} = 2k_3[e][M_e] + k_5[H][M_g] - \left(\frac{2}{d}\right)k_9[R_g][S] \quad (5)$$

$$\frac{d(Q[M_g])}{dV} = -k_3[e][M_g] - k_5[H][M_g] - k_6[R_g][M_g] - \left(\frac{2}{d}\right)k_{10}[M_g][R_s] - \left(\frac{2}{d}\right)k_{11}[M_s][R_s] \quad (6)$$

$$\frac{d(Q[H])}{dV} = 2k_2[e][M_g] + 2k_4[e][H_2] - k_5[H][M_g] - \left(\frac{2}{d}\right)k_8[H][S] \quad (7)$$

$$\frac{d(Q[H_2])}{dV} = k_1[e][M_g] - k_4[e][H_2] + \left(\frac{2}{d}\right)k_8[H][S] \quad (8)$$

The quantity $Q$ appearing on the left-hand sides of eq 5–8 is the total volumetric flow rate. This quantity is not constant in general and will vary with axial position through the discharge. To obtain an expression for the variation of $Q$ with position, we define the molar flow rate $F_j$ of any species $X_j$ as

$$F_j = Q[X_j] \quad (9)$$

and the total molar flow rate $F$ as

$$F = \sum_{j=1}^{4} F_j = Q[N_g] \quad (10)$$

where $[N_g]$ is the total gas concentration. Differentiating $F_j$ and $F$ with respect to $V$ gives

$$\frac{dF_j}{dV} = r_j \quad (11)$$

$$\frac{dF}{dV} = [N_g]\frac{dQ}{dV} = \sum_{j=1}^{4} r_j = r_0 \quad (12)$$

where $r_j$ represents the right-hand side of eq. 5–8. Equation 12 provides the desired relation between $Q$ and $V$.

Equations 11 and 12 can also be used to rewrite eq 5–8 in the form of a system of first-order nonlinear differential equations. The final form of these equations is given by

$$\frac{d[X_j]}{dV} = \frac{[N_g]}{F}\left(r_j - \frac{[X_j]}{[N_g]}r_0\right) \quad (13)$$

The system of equations is solved by standard numerical techniques. In this work, the Adams–Moulton difference scheme[31] was used to calculate $[R_g]$, $[M_g]$, $[H]$, $[H_2]$, and $Q$ as a function of reactor volume, $V$. The boundary conditions at $V = 0$ used in solving these equations were

$$[R_g] = [H] = [H_2] = 0$$
$$[M_g] = [M_g]_0 = [N_g] \quad (14)$$
$$Q = Q_0$$

While it is generally necessary to use numerical methods to solve for the concentrations of radicals and monomer, analytical solutions for these quantities can be found when the extent of monomer conversion is low. Under this circumstance $[H]$, $[H_2]$, and $[R_g]$ will be small compared to $[M_g]$, and $Q$ will remain essentially constant throughout the reactor. Thus, it is possible to neglect the differential equations for $[H_2]$ and $Q$ and to focus only on the equations for $[R_g]$, $[H]$, and $[M_g]$.

A further simplification can be made if we assume no difference between the behavior of hydrogen atoms and free radicals. Introduction of this assumption allows one to neglect eq 7 and to drop the term for reaction 5 from eq 5 and 6. The terms for reactions 6, 10, and 11 will also be dropped from eq 6 since they are expected to contribute in a negligible manner to the depletion of monomer.

Using the simplifications and assumptions just discussed, eq 5 and 6 can be written as

$$Q_0\frac{d[R_g]}{dV} = 2k_3[e][M_g] - \left(\frac{2}{d}\right)k_9[R_g][S] \quad (15)$$

$$Q_0\frac{d[R_g]}{dV} = -k_3[e][M_g] \quad (16)$$

Equations 15 and 16 can be solved together with the boundary conditions given in eq 14 to obtain

$$[M_g] = [M_g]_0 e^{-a\tau} \quad (17)$$

$$[R_g] = [M_g]_0\frac{2a}{(a-b)}(-e^{-a\tau} + e^{-b\tau}) \quad (18)$$

where $a = k_3[e]$; $b = (2/d)k_9[S]$; $\tau = V/Q$. Finally, the rate of polymerization can be written as

$$r_p = \frac{2ca}{(a-b)}[M_g]_0^2\frac{1 - e^{-(a-b)\tau}}{e^{(a+b)\tau}} \quad (19)$$

where $c = (d/2)k_6 + k_{10}K_R + k_{11}K_M K_R$.

The form of eq 19 indicates that the dependence of the polymerization rate on space time, $r_p$, will be influenced strongly by the magnitudes of $a$ and $b$. The constant $c$ affects only the magnitude of the curves of $r_p$ vs. $Q$ but not their shape.

### Comparison with Experiment

The model of plasma polymerization was tested by comparing curves of polymer deposition rate vs. monomer flow rate predicted by the model with those observed experimentally. The experimental results were taken from the work of Kobayashi et al.[29,32] In these studies various hydrocarbons were polymerized by passing a flow of monomer gas through a plasma sustained between two parallel electrodes. Data were gathered using two reactors: the first a bell jar reactor containing circular electrodes and the second a tubular reactor containing rectangular electrodes. Experimental results obtained with both reactors were nearly identical both qualitatively and quantitatively.[33]

Numerical solutions of eq 12 and 13 require knowledge of the magnitude of ten rate coefficients, the electron density, and the concentration of adsorption sites at the polymer surface. A priori assignment of these values is impossible because of the lack of available data. Consequently, the rate coefficients were used as fitting parameters after the following simplifications were introduced. Since the electron density and the concentration of adsorption sites always appear multiplied by a rate coefficient, the products rather than the individual factors were used as the fitting parameters. Furthermore, the initiation coefficients, $k_1$ through $k_4$, were assumed to be equivalent to one another and the adsorption coefficients, $k_8$ and $k_9$, were assumed to be equal. Gas-phase propagation rate coefficients, $k_5$ and $k_6$, were also assumed to be equal. Finally, since it has been argued above that very little monomer adsorbs on the growing polymer surface, $K_M$ was taken to be small and the product $k_{11}K_M K_R$ assumed to be negligible. Introduction of the above simplifications reduces the number of adjustable parameters in the numerical model to four, viz., $k_i[e] = k_1[e] = k_2[e] = k_3[e] = k_4[e]$, $k_{p_g} = k_5 = k_6$, $k_a = k_8[S] = k_9[S]$, and $k_{p_s} = k_{10}K_R$.

Figure 2 illustrates the effect of monomer flow rate on the rate of butadience polymerization. The points represent ex-

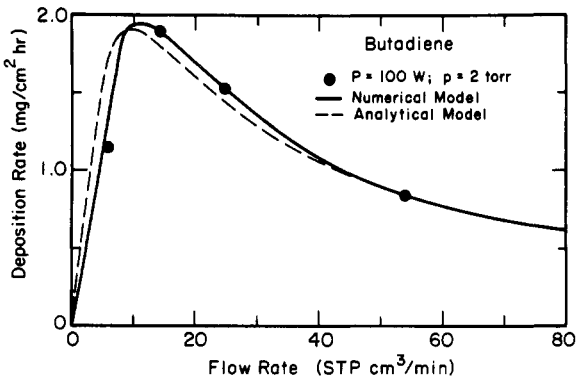


**Figure 2.** Predicted and experimental rates of polymer deposition as a function of monomer flow rate.

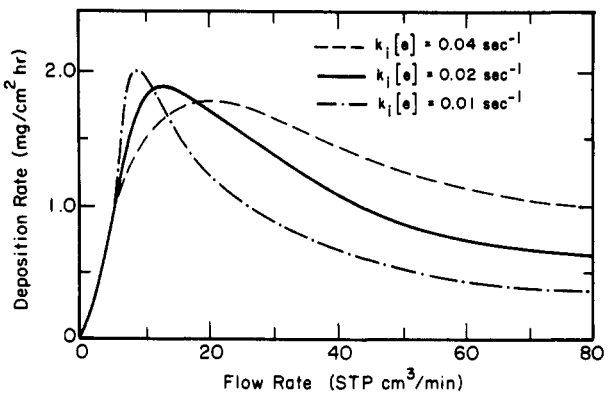


**Figure 3.** Effect of $k_i$[e] on predicted deposition rate curves.

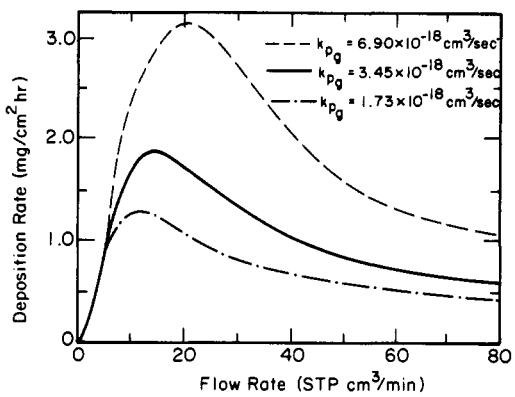


**Figure 4.** Effect of $k_{p_g}$ on predicted deposition rate curves.

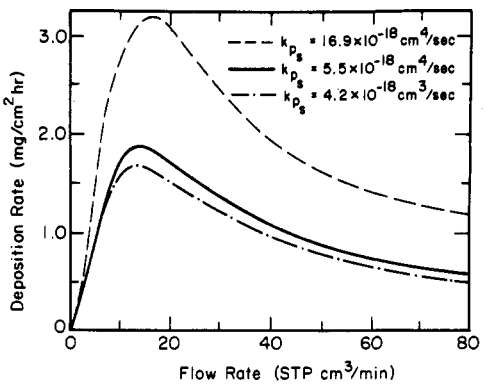


**Figure 5.** Effect of $k_{p_s}$ on predicted deposition rate curves.

perimental data and the solid curve the prediction of the model. A perfect fit is achieved between the computed and measured rates by adjusting the rate coefficients appearing in the model to the following values:

$$k_i[\mathrm{e}] = 2.1 \times 10^{-2}\ \mathrm{s}^{-1}$$

$$k_{p_g} = 3.45 \times 10^{-18}\ \mathrm{cm}^3/\mathrm{s}$$

$$k_a = 7.5 \times 10^{-3}\ \mathrm{cm/s}$$

$$k_{p_s} = 5.5 \times 10^{-18}\ \mathrm{cm}^4/\mathrm{s}$$

The effect on the predicted deposition rate of varying $k_i$[e], $k_{p_g}$, or $k_{p_s}$ by a factor of 2 from the best fit value is shown in Figures 3–5. The primary parameter in determining the shape, but not the magnitude, of the curve describing $r_p$ as a function of $Q$ is $k_i$[e]. Figure 3 shows that the location of the maximum point in the curve of $r_p$ vs. $Q$ as well as the rate of change of $r_p$ with $Q$ are strongly controlled by $k_i$[e]. The parameter $k_{p_g}$, which describes the rate of gas-phase polymerization, has a significant effect on the magnitude of $r_p$ (Figure 4) and a smaller influence on the shape of the deposition curve. Figure 5 shows that the magnitude of $k_{p_s}$ also influences both the magnitude and shape of the deposition rate curve although the effects of changing this parameter are not as significant as those observed for a comparable change in the value of $k_{p_g}$. Variations in the value of $k_a$ in the narrow range between 3.75 $\times 10^{-3}$ and 15.0 $\times 10^{-3}$ cm/s had only a very small effect on the predicted curve of $r_p$ vs. $Q$.

The correspondence between measured and predicted polymerization rates shown in Figure 2 is encouraging but does not guarantee that the mechanism selected to describe the kinetics and the simplifying assumptions is physically correct. An additional step toward supporting the model can be taken by comparing the magnitudes of the fitted rate coefficients with those estimated or measured for similar elementary processes.

The rate coefficients $k_1$ through $k_4$ have not been measured and cannot be estimated reliably. Nevertheless it is possible to compare the value of $k_i$ used in the model with values of dissociation rate coefficients measured for simple molecular gases. To carry out such a comparison it is first necessary to evaluate [e], the electron density. This may be done by recognizing that [e] can be estimated from the relationship[21]

$$[\mathrm{e}] = 5 \times 10^{10} \bar{P} \Lambda \qquad (20)$$

where $\bar{P}$ is the power density in the discharge and $\Lambda = d/\pi$ is the characteristic length of the discharge. For $\bar{P} = 0.1$ W/cm$^3$ and $d = 5$ cm, [e] = $8 \times 10^9$ cm$^{-3}$. Consequently, $k_i = 2.5 \times 10^{-12}$ cm$^3$/s. Dissociation of $O_2$ and $H_2$ by electron collisions is characterized by rate coefficients which are of the order $10^{-11}$ cm$^3$/s.[21] Thus, it is seen that the value of $k_i$ used in the model is in reasonable agreement with the magnitude of rate coefficients for processes similar to reactions 1–4.

The magnitude of $k_{p_g}$ obtained by fitting the data can be compared with the magnitude of the propagation rate coefficient for conventional free-radical polymerization of butadiene. Lenz[34] reports a value of $3.7 \times 10^{-18}$ cm$^3$/s which is in excellent agreement with our value of $3.45 \times 10^{-18}$ cm$^3$/s. This level of consistency gives strong support to the proposition that gas-phase oligomerization occurs via a free-radical mechanism.

Published values for rate coefficients characterizing free-radical adsorption onto a polymer surface are not available for comparison with $k_a$. However, it is possible to explore whether or not the fitted value of $k_a$ is physically reasonable by using absolute rate theory to estimate $k_a$. Assuming that the rate of free-radical adsorption is limited by collisions between gas-phase free radicals and the growing polymer surface and that the fraction of the surface available for adsorption is essentially unity, a value of $k_a = 10$ cm/s is estimated.[35,36] This value is about a factor of $10^3$ larger than that used to obtain a fit to the experimental data ($k_a = 7.5 \times 10^{-3}$ cm/s).

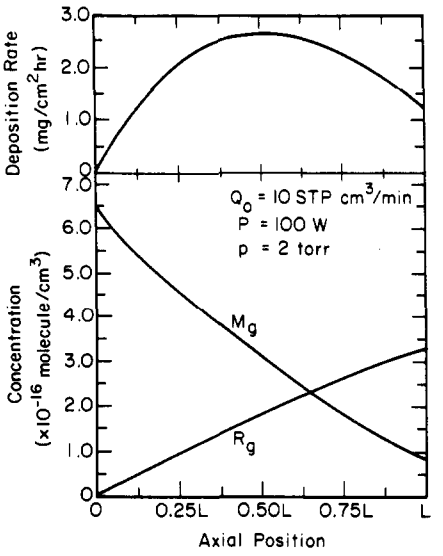


**Figure 6.** Numerical model predictions of polymer deposition rate and monomer and free-radical concentrations as a function of axial position for butadiene polymerization.

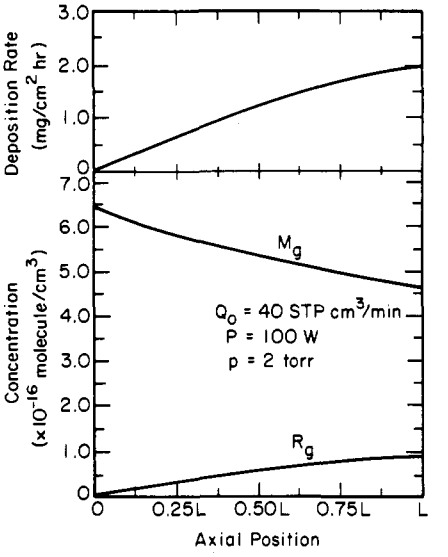


**Figure 7.** Numerical model predictions of polymer deposition rate and monomer and free-radical concentrations as a function of axial position for butadiene polymerization.

The large difference between the estimated and fitted values of $k_a$ possibly could be explained if desorption of adsorbed radicals occurred almost as rapidly as adsorption. Under such circumstances the fitted value of $k_a$ would describe the net rate of radical adsorption, which could be substantially smaller than the absolute rate of adsorption.

It is important to note here that it is unlikely that the transport of free radicals from the plasma to the growing polymer surface is rate limited by diffusion. For a pressure of 1 Torr a reasonable value of the diffusion coefficient $D$ is $10^2$ cm$^2$/s. Assuming an average diffusion distance of $d/2 = 2.5$ cm we arrive at a diffusion velocity of 40 cm/s. This value is also considerably greater than the fitted value of $k_a$. Correspondingly, one expects the adsorption of free radicals to be rate limited by kinetic processes occurring at the growing polymer surface.

Independent estimates of $k_{p_s}$ cannot be obtained since this coefficient is the product of a rate coefficient $k_{10}$ and a proportionality coefficient $K_R$. The latter quantity is not identified clearly with an elementary process and hence cannot be estimated theoretically.

Further insight into the details of the polymerization kinetics can be obtained by inspection of the deposition rate and monomer and free-radical concentrations as a function of position in the discharge zone. Figures 6 and 7 illustrate such curves for two monomer flow rates. At a flow rate of 10 STP cm$^3$/min, the residence time is sufficient for significant radical concentrations to be established within a short distance from the entrance to the discharge zone. This results in a rapid increase in the polymerization rate. The passage of the polymerization rate through a maximum and its subsequent decline are due to a depletion of monomer which occurs toward the exit end of the discharge zone. For a flow rate of 40 STP cm$^3$/min the monomer concentration does not decline significantly with position in the discharge. Under these circumstances the polymerization rate increases with increasing distance through the discharge zone, in line with the rate of change of the radical population, as shown in Figure 7. Experimental observations of polymer thickness profiles which are consistent with the predictions of the present model have been reported by Kobayashi et al.[33]

The rate expression based upon the analytical solution to eq 15 and 16 can also be fitted to the experimentally measured rates of butadiene polymerization. The result is given by the dashed curve in Figure 2. For these calculations the following

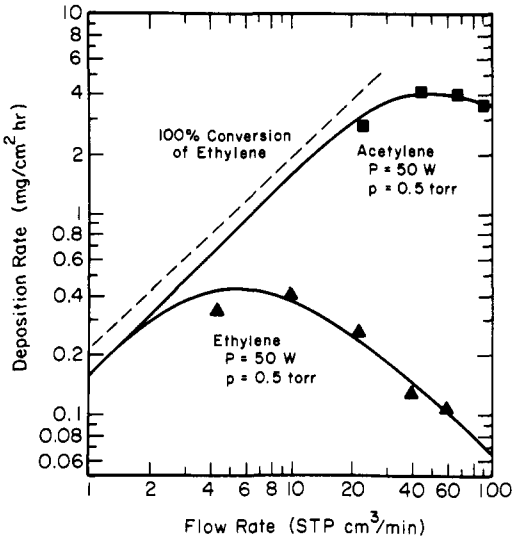


**Figure 8.** Predicted and experimental deposition rates as a function of monomer flow rate.

values of the rate coefficients were used

$$k_i[e] = 8.0 \times 10^{-2}\ s^{-1}$$

$$k_a = 7.5 \times 10^{-3}\ cm/s$$

$$(d/2)k_{p_g} + k_{p_s} = 10^{-18}\ cm^4/s$$

It should be noted that the value of $k_i[e]$ used with the analytical model is about four times as large as that used with the numerical model. The reason for this is that $k_i[e]$ represents the sum of $k_2[e]$ and $k_3[e]$ since the analytical model makes no distinction between the production of hydrogen atoms and free radicals. It should also be observed that the sum $((d/2)k_{p_g} + k_{p_s})$ is smaller for the analytical model than for the numerical model.

Figure 8 compares the rates of ethylene and acetylene polymerization predicted by the analytical model with experimentally measured rates.[32] For both monomers a good fit to the data can be obtained by adjusting the values of $k_i[e]$ and $((d/2)k_{p_g} + k_{p_s})$ while holding the value of $k_a$ constant. It is noted in Table II that the values of $k_i[e]$ and $((d/2)k_{p_g} + k_{p_s})$ are larger for acetylene than for ethylene. This ordering suggests that the rate of free-radical formation via electron

**Table II**
**Fitted Rate Coefficients Obtained from the Analytical Model**

| Monomer | Pressure, Torr | Power, W | $k_i[e]$, $s^{-1}$ | $(2/d)k_a$, $s^{-1}$ | $(d/2)k_{pg} + k_{ps}$, $cm^4/s$ |
|---|---|---|---|---|---|
| Acetylene | 0.5 | 50 | 1.75 | $3.2 \times 10^{-3}$ | $2.45 \times 10^{-16}$ |
| Ethylene | 0.5 | 50 | 0.18 | $3.2 \times 10^{-3}$ | $2.40 \times 10^{-17}$ |
| Isobutylene | 2.0 | 100 | 0.030 | $3.2 \times 10^{-3}$ | $4.60 \times 10^{-19}$ |
| Propylene | 2.0 | 100 | 0.030 | $3.2 \times 10^{-3}$ | $1.45 \times 10^{-18}$ |
| Butadiene | 2.0 | 100 | 0.08 | $3.2 \times 10^{-3}$ | $3.65 \times 10^{-18}$ |
| Ethylene | 2.0 | 100 | 0.10 | $3.2 \times 10^{-3}$ | $7.70 \times 10^{-18}$ |
| Ethylene | 0.7 | 100 | 0.22 | $3.2 \times 10^{-3}$ | $2.90 \times 10^{-17}$ |
| Ethylene | 2.0 | 100 | 0.10 | $3.2 \times 10^{-3}$ | $7.70 \times 10^{-18}$ |
| Ethylene | 0.5 | 50 | 0.18 | $3.2 \times 10^{-3}$ | $2.40 \times 10^{-17}$ |

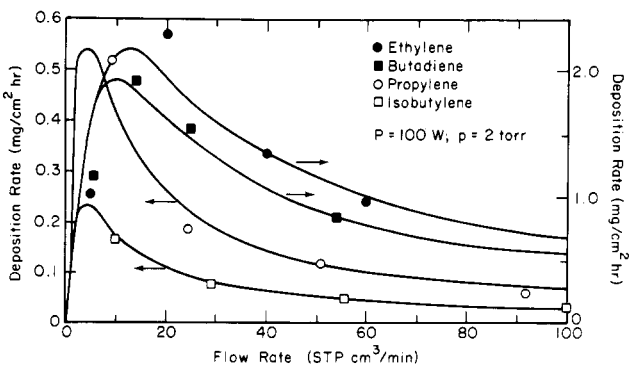


**Figure 9.** Predicted and experimental deposition rates for olefins as a function of monomer flow rate.

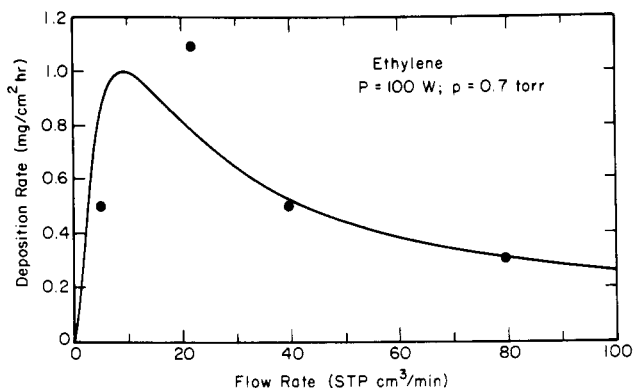


**Figure 11.** Predicted and experimental ethylene deposition rates as a function of monomer flow rate.

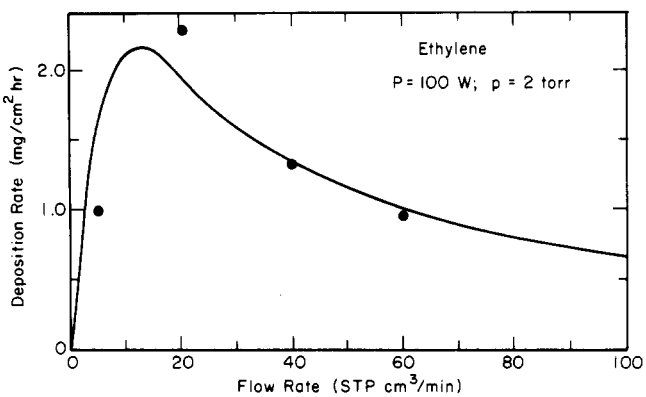


**Figure 10.** Predicted and experimental ethylene deposition rates as a function of monomer flow rates.

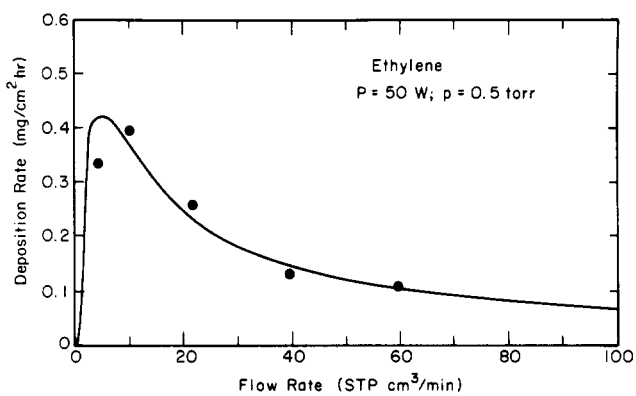


**Figure 12.** Predicted and experimental ethylene deposition rates as a function of monomer flow rate.

impact and the subsequent addition of monomer to both gas phase and surface free radicals occur more rapidly for acetylene.

Additional tests of the analytical model were performed by using it to fit experimental data for the plasma polymerization of ethylene, butadiene, propylene, and isobutylene.[30] The results are shown in Figure 9 and the rate coefficients required to achieve the observed fit are tabulated in Table II. From an inspection of Table II it is apparent that monomers which polymerize rapidly exhibit large values of $k_i[e]$ and $((d/2)k_{pg} + k_{ps})$. A satisfactory explanation of the observed trend in ease of polymerization cannot be offered at this time.

The effects of changes in pressure and discharge power on the rate of ethylene polymerization are shown in Figures 10–12. The solid curves appearing in those figures again represent predictions of the polymerization rate based upon the analytical model. Examination of the values of $k_i[e]$ obtained by forcing agreement between theory and experiment shows several interesting trends. To begin with, we notice that at 100 W the value of $k_i[e]$ decreases as the pressure is increased from 0.7 to 2.0 Torr. This change is in agreement with what would be expected on the basis of electric discharge theory.[21] As the pressure increases the value of $E/P$, the ratio of the electric field sustaining the plasma to the gas pressure, decreases and causes decrease in the average electron energy. The decrease in electron energy in turn causes a reduction in the rate coefficient of all electron–molecule collision processes. A further consequence of an increase in pressure is a decrease in electron density.[21] Taken together, the effect of an increase in pressure is to cause $k_i[e]$ to decrease.

Electric discharge theory may also be used to determine the expected consequences of an increase in discharge power. In this instance a linear relationship between electron density and power is anticipated, provided the gas pressure is held constant. Such an effect should cause the value of $k_i[e]$ to increase linearly with power. Comparison of the values of $k_i[e]$ used to fit the data in Figures 11 and 12 shows that $k_i[e]$ in-

creases with power but does not double as would be expected. This may be explained by the fact that the pressure associated with Figure 11 is 40% higher than that associated with Figure 12. As discussed earlier, increasing pressure causes a decrease in the value of $k_i$[e]. As a result it is quite conceivable that the increase in $k_i$[e] due to increased power is partially offset by the concurrent increase in pressure.

Conclusions can also be drawn by comparing the values of $((d/2)k_{p_g} + k_{p_s})$ used to compute the theoretical curves appearing in Figures 10–12. The value of this group is essentially the same for the conditions corresponding to Figures 10 and 12. This is as expected since neither power nor pressure should influence the magnitude of the polymerization rate coefficients. The nearly threefold decrease in the value of $((d/2)k_{p_g} + k_{p_s})$ required to describe the data in Figure 11 is unexpected and cannot be readily explained. The observed change may signify that at 2 Torr the simple analytical expression is no longer an accurate physical representation of the kinetics.

## Conclusion

A general mechanism for the polymerization of unsaturated hydrocarbon monomers in a glow discharge has been presented. Initiation is assumed to occur as a result of electron–molecule collisions which lead to the formation of free-radical reaction intermediates in the gas phase. These species undergo addition reactions with the monomer, both in the gas phase and on surfaces, following adsorption of the radicals. The rate of polymerization, which is the sum of gas phase and surface propagation steps, was determined by solving material balance equations which described the free radical and monomer concentrations as a function of axial position in a flow reactor. In general, numerical solution of these equations was required, but an analytical solution was also obtained for low monomer conversions.

Reaction rate coefficients were used as fitting parameters in comparing the model predictions to experimental deposition rate data. Good agreement between the data and both the numerical and analytical model predictions was observed. Furthermore, the fitted rate coefficients describing initiation and gas-phase oligomerization were in good quantitative agreement with independently observed rate coefficients. The model shows that the magnitude of the initiation rate coefficient is the primary parameter in determining the shape of the deposition rate vs. flow rate curve. By contrast, the propagation rate coefficients have a less significant effect on the magnitude of the predicted rate.

It has been shown that the magnitudes of the fitted initiation and polymerization rate constants correlate with the relative reactivity of a given monomer. Rapid polymerization is exhibited by monomers having large values of these two coefficients. Finally, the predicted rate coefficients change in agreement with what would be expected on the basis of electric discharge theory when gas pressure and discharge power are varied.

It is recognized that the ability of the proposed model to describe experimental data does not in and of itself justify the many assumptions introduced in order to bring the mathematical formalism into a tractable form. Nevertheless, the good quantitative agreement between the fitted and independently observed rate coefficients for the initiation and propagation processes strongly supports, in our opinion, the proposition that plasma polymerization, conducted under conditions similar to those considered here, occurs predominately by a free-radical mechanism. This conclusion does not exclude the possibility that at significantly lower pressures where ion and free-radical concentrations are more nearly equal that ionic processes might begin to contribute to the polymerization kinetics.

**Acknowledgment.** The authors wish to acknowledge the support of this work by the NSF through Grant GH-43410.

## References and Notes

(1) P. J. Ozawa, *IEEE Trans. Parts, Mater. Packag.*, **5**, 112 (1969).
(2) R. W. Kirk, "Techniques and Applications of Plasma Chemistry", J. R. Hollahan and A. T. Bell, Ed., Wiley, New York, N.Y., 1974.
(3) H. Yasuda and C. E. Lamaze, *J. Appl. Polym. Sci.*, **17**, 201 (1973).
(4) A. T. Bell, T. Wydeven, and C. C. Johnson, *J. Appl. Polym. Sci.*, **19**, 1911 (1975).
(5) A. F. Stancell and A. T. Spencer, *J. Appl. Polym. Sci.*, **16**, 1505 (1972).
(6) T. Wydeven and J. R. Hollahan, ref 2.
(7) K. Tien, G. Smolinsky, and R. J. Martin, *Appl. Opt.*, **11**, 637 (1972).
(8) J. R. Hollahan, T. Wydeven, and C. C. Johnson, *Appl. Opt.*, **13**, 184[4] (1974).
(9) I. Haller and P. White, *J. Phys. Chem.*, **67**, 1784 (1963).
(10) T. Williams and M. W. Hayes, *Nature (London)*, **216**, 614 (1967).
(11) A. F. Denaro, P. A. Owens, and A. Crawshaw, *Eur. Polym. J.*, **4**, 93 (1968).
(12) A. R. Denaro, P. A. Owens, and A. Crawshaw, *Eur. Polym. J.*, **5**, 471 (1969).
(13) H. Yasuda and C. E. Lamaze, *J. Appl. Polym. Sci.*, **15**, 2277 (1971).
(14) L. F. Thompson and K. G. Mayhan, *J. Appl. Polym. Sci.*, **16**, 2317 (1972).
(15) L. F. Thompson and K. G. Mayhan, *J. Appl. Polym. Sci.*, **16**, 2291 (1972).
(16) M. Duval and A. Theoret, *J. Appl. Polym. Sci.*, **17**, 527 (1973).
(17) H. Carchano, *J. Chem. Phys.*, **61 (9)**, 3634 (1974).
(18) D. K. Lam, R. F. Baddour, and A. F. Stancell, *J. Macromol. Sci., Chem.*, **10**, 421 (1976).
(19) H. U. Poll, M. Arzt, and K. H. Wickleder, *Eur. Polym. J.*, **12**, 505 (1976).
(20) G. Smolinsky and M. J. Vasile, *J. Macromol. Sci., Chem.*, **10**, 473 (1976).
(21) A. T. Bell, ref 2.
(22) A. T. Bell, *Ind. Eng. Chem., Fundam.*, **11**, 209 (1972).
(23) L. C. Brown and A. T. Bell, *Ind. Eng. Chem., Fundam.*, **13**, 210 (1974).
(24) A. T. Bell, *J. Macromol. Sci., Chem.*, **10**, 369 (1976).
(25) H. Kobayashi, M. Shen, and A. T. Bell, *J. Macromol. Sci., Chem.*, **8**, 1345 (1974).
(26) N. Morosoff, B. Crist, M. Bumgarner, T. Hsu, and H. Yasuda, *J. Macromol. Sci., Chem.*, **10**, 451 (1976).
(27) S. Morita, T. Migutani, and M. Ieda, *Jpn., J. Appl. Phys.*, **10**, 1275 (1971).
(28) A. Bradley and D. Fales, *Chem. Technol.*, 232 (April 1971).
(29) H. Kobayashi, M. Shen, and A. T. Bell, *J. Macromol. Sci., Chem.*, **8 (2)**, 373 (1974).
(30) P. J. Flory, "Principles of Polymer Chemistry", Cornell University Press, Ithaca, N.Y., 1953.
(31) C. Risk, Technical Report No. 44, Computer Center, University of Calif., Berkeley, Calif., 1974.
(32) H. Kobayashi, A. T. Bell, and M. Shen, *Macromolecules*, **7**, 277 (1974).
(33) H. Kobayashi, A. T. Bell, and M. Shen, *J. Macromol. Sci., Chem.*, **10**, 491 (1976).
(34) R. W. Lenz, "Organic Chemistry of Synthetic High Polymers", Wiley, New York, N.Y., 1967.
(35) K. J. Laidler, "Chemical Kinetics", McGraw-Hill, New York, N.Y., 1965.
(36) J. M. Tibbitt, Ph.D. Thesis, Department of Chemical Engineering, University of California, Berkeley, Calif., 1975.